

## Part VI

# Distant Hot Gas, SXR B Fluctuations, Dust, $\gamma$ -rays



Different points of view during the coffee break ...



... and the Wednesday afternoon excursion to Nymphenburg Castle.

# Modeling the Galactic $\frac{3}{4}$ keV X-ray Background

M.J. Freyberg and J.H.M.M. Schmitt

Max-Planck-Institut für extraterrestrische Physik, D-85740 Garching, Germany

**Abstract.** We have analyzed the ROSAT PSPC all-sky survey maps of the soft X-ray background (SXRb) in the  $\frac{3}{4}$  keV band. One approach was to study the large-scale distribution of the X-ray emission with a multipole analysis. Here a significant dipole toward the galactic center region was found. This is interpreted in terms of variation of distant X-ray emission, e.g. galactic halo. Also a small-scale structure analysis of the  $\frac{3}{4}$  keV X-ray sky has been performed and a new analytic fluctuation probability distribution has been derived. No significant excess over the expected extragalactic point source contribution has been found. Finally, X-ray colours have been used to investigate spectral variations of the SXRb.

## 1 Introduction

At energies above approximately 2 keV most of the observed X-ray background is certainly of extragalactic origin except for a rather narrow galactic ridge seen out to energies of a few keV (cf. Worrall et al. 1982), while in the  $\frac{1}{4}$  keV band a major fraction of the X-rays originates within the next hundred parsec (e.g., the reviews by McCammon & Sanders 1990, Fabian & Barcons 1992, Breitschwerdt et al. 1996). At energies around and above 1 keV the decomposition of the diffuse background into galactic and extragalactic components is much less clear. Extrapolating from the  $\frac{1}{4}$  keV band and from higher energies into the  $\frac{3}{4}$  keV band an excess is found. However, at high galactic latitudes where “deep surveys” with imaging X-ray telescopes have traditionally been performed (cf. Giacconi et al. 1979, Hasinger et al. 1993), the dominant background component is still of extragalactic origin (cf. Schmitt & Snowden 1990).

In the following a report is given on the analysis of the ROSAT  $\frac{3}{4}$  keV band. The distance to the origin of the detected soft X-rays is related to their energy as the interstellar absorption cross section varies as  $E^{-8/3}$  (away from absorption edges). The higher the energy the more distant emission is detected with ROSAT. Table 1 summarizes the relation of the optical depth  $\tau = 1$  for various ROSAT PSPC energy bands for Raymond-Smith-type plasma with  $\log T$  [K] = 6.0–6.4. Abundances of cold and hot matter used in our modeling were according to Morrison & McCammon (1983) and Raymond & Smith (1977), respectively.

Band	Channels	Column density for $\tau = 1$		
R1	8 – 19	8 – 10.5	×	$10^{19} \text{ cm}^{-2}$
R2	20 – 41	1 – 1.5	×	$10^{20} \text{ cm}^{-2}$
R4	52 – 69	6 – 12	×	$10^{20} \text{ cm}^{-2}$
R5	70 – 90	1 – 1.5	×	$10^{21} \text{ cm}^{-2}$
R6	91 – 131	1.8 – 2.7	×	$10^{21} \text{ cm}^{-2}$
R7	132 – 201	3 – 6	×	$10^{21} \text{ cm}^{-2}$

**Table 1.** Optical depth  $\tau = 1$  for various energy bands for Raymond-Smith-type plasma with  $\log T [\text{K}] = 6.0 - 6.4$  for the ROSAT PSPC. The PSPC channels multiplied with 10 eV give the approximate energies.

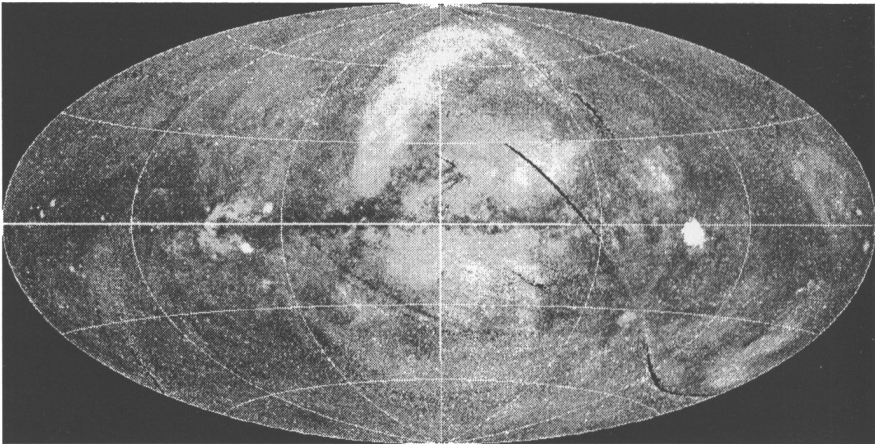


**Fig. 1.** RGB image of the SXRb using the new survey maps (Snowden et al. 1997). The three energy bands, 1/4, 3/4, and 1.5 keV, are colour-coded with red, green, and blue, respectively. As in all our maps we use galactic coordinates with increasing longitudes to the left and  $l = 0^\circ$  in the center; (see Plate 3).

## 2 X-ray Colours

One way to characterize spectral parameters of X-ray emission is in terms of X-ray colours. This is especially useful for soft X-rays as the absorption cross section strongly depends on energy (Tab.1). Figure 1 shows a 3-colour map of the ROSAT PSPC all-sky survey. Three energy bands, 1/4, 3/4, and 1.5 keV, are colour-coded with red, green, and blue, respectively. At higher galactic latitudes soft emission dominates while in the galactic plane this band is highly absorbed and only hard X-rays are present.

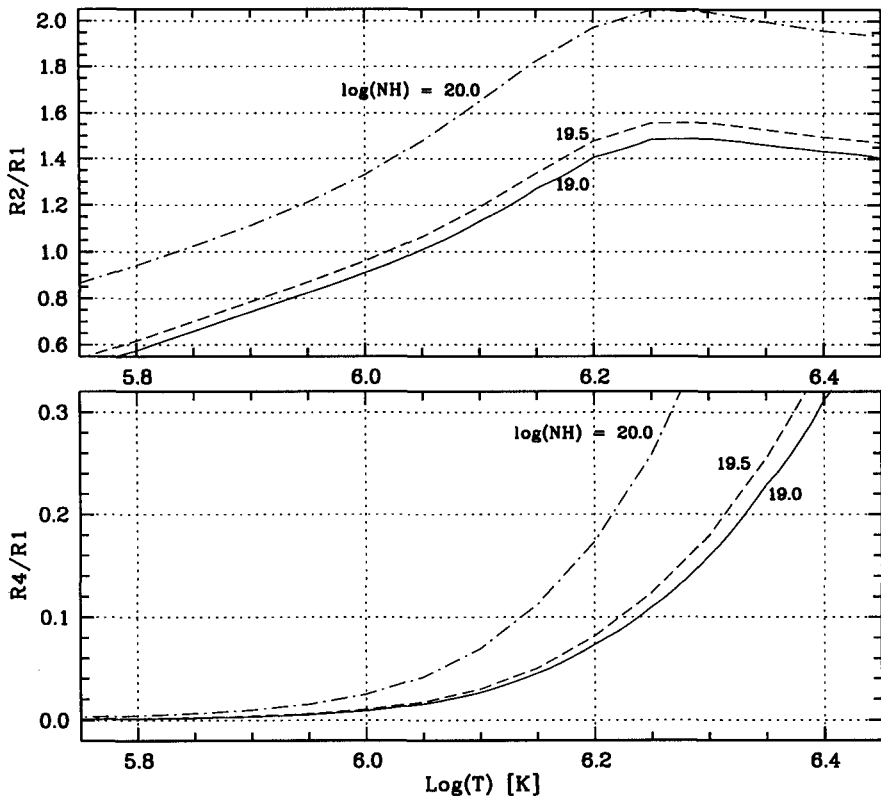
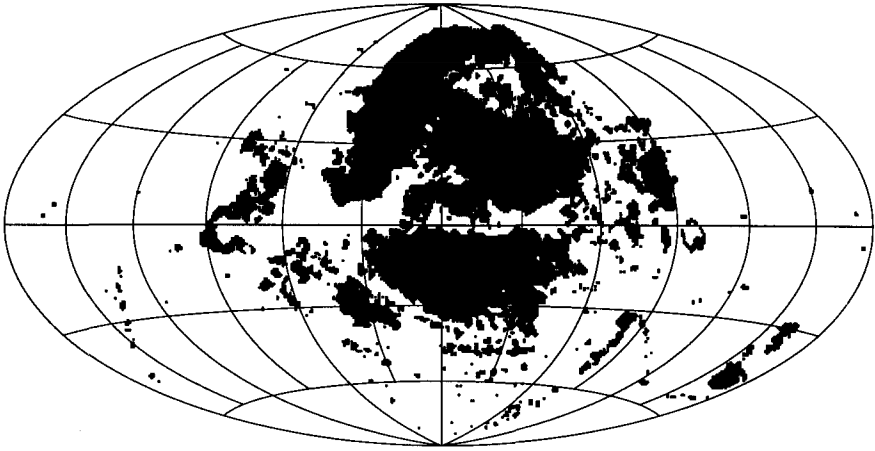


Fig. 2. a) R2/R1 ratio as a function of plasma temperature for three representative column densities  $N_H$ . b) R4/R1 ratio similar to above.

The ratio of the Wisconsin B and C band survey maps showed only small variations of C/B with large variations of absorbing neutral hydrogen column densities  $N_H$  (McCammon et al. 1983). This led to the conclusion that most (if not all) X-rays in the 1/4 keV band originate in front of the bulk of absorbing matter. For the ROSAT PSPC corresponding bands are the R1 and R2 band, respectively. In Fig.2a we show the dependence of R2/R1 as a function of plasma temperature for 3 column densities,  $\log N_H [\text{cm}^{-2}] = 19.0, 19.5, 20.0$ . Similarly, Fig.2b gives the ratio R4/R1 for these column densities. Snowden et al. (1998) discuss the R2/R1 ratio in detail and try to disentangle local and distant contributions to the 1/4 keV band.

The R4/R1 ratio is compared to the R2/R1 ratio more sensitive to distant emission. While a typical value for R2/R1 is 1.1 (consistent with  $\log T [\text{K}] \sim 6.05$  and  $\log N_H [\text{cm}^{-2}] \sim 19.5$ ), an average R4/R1 at low galactic latitudes in the galactic anti-center direction is 0.13. This is not consistent with a low local temperature, but would require  $\log T [\text{K}] > 6.25$ . At the moment



**Fig. 3.** Distribution of regions with  $R1 < 100 \times 10^{-6} \text{ cts s}^{-1} \text{ arcmin}^{-2}$  and  $R4 > 80 \times 10^{-6} \text{ cts s}^{-1} \text{ arcmin}^{-2}$ . A median filter had been applied to the maps.

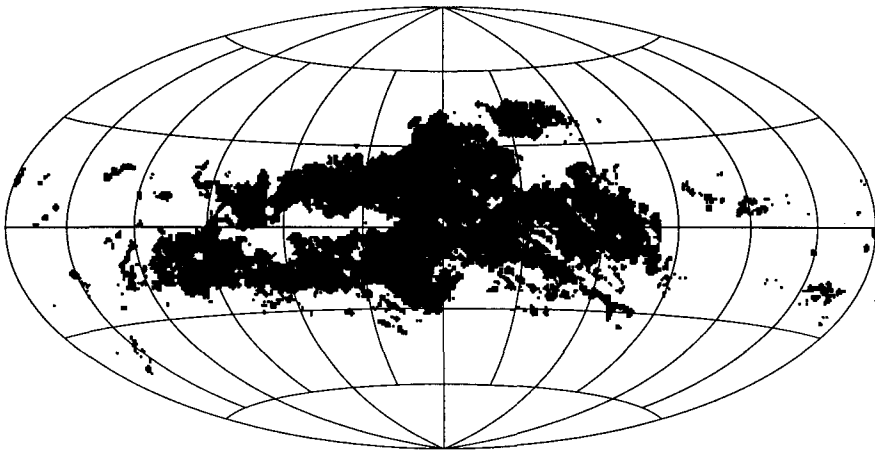


**Fig. 4.** Distribution of regions with  $R1 < 200 \times 10^{-6} \text{ cts s}^{-1} \text{ arcmin}^{-2}$  and corrected (local bubble subtracted, residual de-absorbed)  $R4 > 50 \times 10^{-6} \text{ cts s}^{-1} \text{ arcmin}^{-2}$ .

X-ray shadows in the 3/4 keV band – e.g. MBM 12 (Kuntz et al. 1997) – do not rule out such a high local temperature, however, they are also not inconsistent with  $\log T [\text{K}] \sim 6.25$ . Or phrased differently, observational data do not rule out either possibility of local or distant origin of the galactic R4 (and R5) band emission. If the 3/4 keV background were merely due to point-like sources (e.g., variations in the extragalactic spectrum or galactic source population), then these could be traced by a fluctuation analysis (cf. Sect.4). The overall spatial distribution of the 3/4 keV emission is discussed

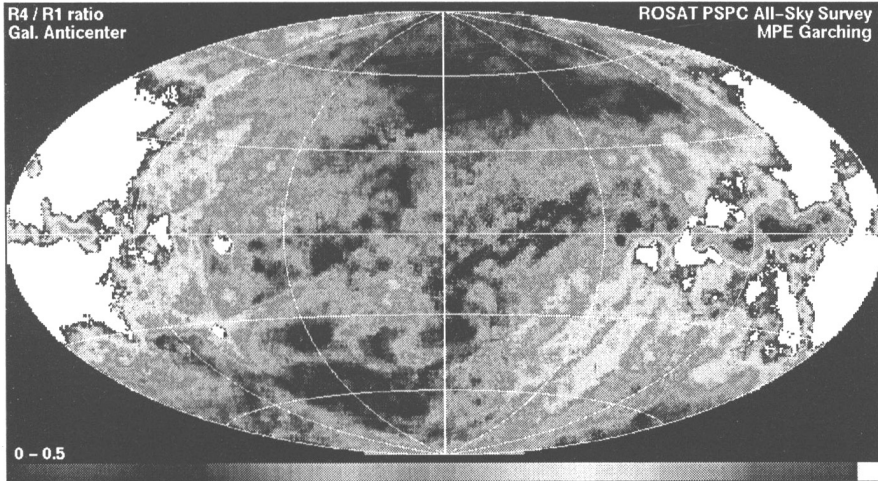


**Fig. 5.** R4/R1 ratio centered at  $l = 180^\circ$ , the colour bar ranges from 0.0 to 0.5; (see Plate 4).

in Sect.3, where variations are most likely due to a hot galactic halo. Using the R4/R1 ratio spectral changes in the soft X-ray background (SXR) are visible, which may reflect spatial emission variations but may also be explained by a non-isothermal distant component (like in the model by Wang 1997). In Fig.3 we show the part of the sky that shows low R1 with  $R1 < 100$  but high R4 with  $R4 > 80$ . Snowden et al. (1997) interpret this component as galactic bulge emission. If we assume a standard local (hot bubble) model with  $\log T [\text{K}] \sim 6.05$ , and subtract local contributions and de-absorb the residual emission for galactic absorption we obtain a map like in Fig.4. Here the points denote regions with  $R1 < 200$  and  $R4_{\text{mod}} > 50$  (where  $R4_{\text{mod}}$  denotes the local bubble subtracted and de-absorbed R4 intensity). Obviously, this is still concentrated toward the galactic center, but extends also into the second quadrant. The region at  $l \sim 240^\circ$  seems to lack R4 band emission. The Sco-Cen superbubble contributes to the northern central region ( $l^{\text{II}} > 20^\circ$ ). Assigning the structure of X-ray colours to a distant hot plasma this can be converted into temperatures of  $\log T [\text{K}] \sim 6.35$ . Finally, Fig.5 shows a sky map of the R4/R1 ratio centered on  $l = 180^\circ$ , where the spectral change from center to anti-center can clearly be seen.

### 3 Large-Scale Structure: Harmonic Analysis

To characterize the large-scale structure of the SXR the intensity distribution can be expanded in spherical harmonics. The strengths of the individual orders then gives information about isotropic (monopole, e.g. extragalactic

background) and non-isotropic components (dipole, quadrupole, etc.). Such a dipole was found in a harmonic analysis of the ratio of the Wisconsin C and B band survey maps (Snowden et al. 1990): this colour gradient was found to be oriented in the galactic plane, one possible interpretation was in terms of a plasma temperature gradient from the galactic anti-center ( $\log T$  [K]  $\sim 5.9$ ) towards the galactic center region ( $\log T$  [K]  $\sim 6.2$ ). Here we follow their approach and apply the same method on the ROSAT 3/4 keV band.

We expand a function  $g$  into a set of orthogonal basis functions. Let  $g(\theta, \phi)$  be a function on the unit sphere, then

$$g(\theta, \phi) = \sum_{l=0}^{\infty} \sum_{m=-l}^{m=+l} A_{lm} Y_{lm}(\theta, \phi). \quad (1)$$

Here  $Y_{lm}(\theta, \phi)$  denote the normalized spherical harmonics (e.g., Abramowitz & Stegun 1965) and  $A_{lm}$  complex coefficients.  $l = 0$  describes a monopole,  $l = 1$  a dipole and so forth. We want to fit a model (certain orders  $l$ ) to a measured quantity  $g(\theta, \phi)$  such as the ROSAT 3/4 keV corrected count rate. This fit is performed by minimizing  $\chi^2$ ,

$$\chi^2 = \int \frac{d\Omega}{\sigma^2(\theta, \phi)} \left[ g(\theta, \phi) - \sum_{l=0}^{L_{\max}} \sum_{m=-l}^{m=+l} A_{lm} Y_{lm}(\theta, \phi) \right]^2. \quad (2)$$

The integration over the solid angle turns into a sum in case of a discrete quantity  $g(\theta, \phi)$ . The weight functions  $\sigma(\theta, \phi)$  contain statistical and systematic uncertainties.  $L_{\max}$  is the maximum multipole order to be considered. Using real  $g(\theta, \phi)$  only  $A_{lm}$  with  $m \geq 0$  are independent quantities. We use galactic coordinates  $\phi = l^{\text{II}}$  and  $90^\circ - \theta = b^{\text{II}}$ . Equation (2) can be solved by inversion of a matrix of order  $(L_{\max} + 1)^2$  (see also Snowden et al. 1990; Freyberg 1994, 1996).

We excluded all those regions of the sky that appeared to be non-typical for the SXRb (e.g., North Polar Spur, Cygnus, Vela) as well as the galactic plane, the galactic center and anti-center regions. Also a minor foreground contribution has been subtracted. To suppress small-scale effects larger spatial bins have been chosen ( $\sim 7 - 28 \text{ deg}^2$ ). In the 3/4 keV band a significant dipole (strength  $\leq 10\%$ ) has been found in the general direction of the galactic center,  $l^{\text{II}} \sim 345^\circ$ ,  $b^{\text{II}} \sim +6^\circ$  (note, that this region had been excluded). The dipole was very stable against further omissions of regions in the fitting procedure. This may be interpreted in terms of a large-scale temperature gradient in the *local* component like in Snowden et al. (1990). However, one can also assume *distant* origin and assign this dipole to a galactic X-ray halo. Higher multipole moments could in principle constrain the shape of such a halo. Unfortunately, quadrupole and even higher moments seem to have reached the noise level which means that these contributions may be affected by small-scale fluctuations like unresolved sources, dim supernova remnants etc. Moreover, no formally acceptable fits could be achieved ( $\chi_{\text{red}}^2 > 5$ ) which

could be caused by an underestimation of systematic effects (and thus too small uncertainties  $\sigma$ ). In a similar analysis the 1.5 keV band data did not show any significant dipole, all moments but the monopole were of approximately equal strength. This may be caused by the intrinsically high fraction of small-scale structure due to the presence of extragalactic sources.

## 4 Small-Scale Structure: Fluctuation Analysis

### 4.1 Introduction

The usual approach in studies to determine the nature of the diffuse X-ray background is to image a fraction of the sky to very low flux levels, to detect and identify all X-ray sources and to construct the so-called  $\log N - \log S$  function, i.e. the cumulative distribution function of the number of sources per steradian with fluxes in excess of  $S$ , i.e.  $N(> S)$ . Integration of  $\frac{dN(>S)}{dS}$  then yields the contribution of the detected sources to the total background.

Having exploited the information contained in the detected sources the question remains whether the not detected can provide any additional information. This problem was first studied by radio astronomers; within rather large beams of the radio telescopes used at that time there would typically be more than one source. Scheuer (1957) developed a formalism how to retrieve information on the number density of sources below the detection limit. The basic idea here is to look at the background fluctuation spectrum. If the background is made up of many individually faint sources, the background fluctuation spectrum will be quite different from the case when the background is made up of a relatively smaller number of stronger sources. Later, the same formalism was applied to X-ray astronomy by Scheuer (1974). Following Freyberg (1994) a fully analytic computation method is presented to study fluctuations in the diffuse galactic SXRb assuming a power-law source luminosity distribution.

### 4.2 The Fluctuation Probability Distribution

Let a source population with a cumulative flux distribution of the form

$$N(> S) = K (S/S_0)^{-\beta} \quad (3)$$

be given, where  $N(> S)$  denotes the number of sources per steradian with flux exceeding the level  $S$ ,  $S_0$  is an arbitrary flux constant,  $\beta$  is the power law index, and  $K$  a normalization constant. The integrated flux  $\Phi(> S)$  of sources with flux exceeding  $S$  and distributed as in Eq.(3) is given by

$$\Phi(> S) = \int_S^\infty d\tilde{S} \tilde{S} \nu(\tilde{S}) \quad (4)$$

with the differential relation  $\nu(S) \sim \frac{dN(>S)}{dS}$ . Inserting Eq.(3) we obtain

$$\Phi(> S) = S_0 K \frac{\beta}{\beta - 1} (S/S_0)^{1-\beta}. \tag{5}$$

Clearly,  $\Phi(> S)$  diverges at faint flux levels (Olbers paradox), and therefore Eq.(3) must cut off at some flux level  $S_{\text{cut}}$ . If the diffuse cosmic X-ray background flux  $\Phi_{\text{cosm}}$  per steradian were known and assumed to be entirely composed of discrete sources, the required cutoff flux could be calculated from  $\Phi(> S_{\text{cut}}) = \Phi_{\text{cosm}}$ ,

$$S_{\text{cut}} = S_0 \left( \frac{\beta - 1}{\beta} \frac{\Phi_{\text{cosm}}}{K S_0} \right)^{1/(1-\beta)}. \tag{6}$$

In applications of X-ray astronomy the fundamental observable is not the X-ray flux, but the (integer) number of counts  $n$  measured in an effective exposure time  $t_{\text{eff}}$  and an effective solid angle  $\Omega_{\text{eff}}$ . We assume  $n$  to be Poisson distributed with some (real) mean  $C_{\text{exp}}$ . Depending on the prevailing instrument characteristics and source spectrum a (single) source with flux  $S$  gives rise to  $C_{\text{exp}} = S t_{\text{eff}} f$  with a suitable flux-to-count conversion factor  $f$ . Hence Eq.(3) can be immediately expressed as

$$N(> C) = K \Omega_{\text{eff}} (C/C_0)^{-\beta}, \tag{7}$$

with  $N(> C)$  denoting the number of sources in the solid angle  $\Omega_{\text{eff}}$  with an expected number of counts in excess of  $C$  and  $C_0 = S_0 t_{\text{eff}} f$ . The expected number of counts in a given beam is given by the superposition of sources distributed according to Eq.(7). The probability distribution of such a sum of random variables, i.e., the fluctuation spectrum, can be most easily calculated with characteristic functions (cf., Scheuer 1957, Scheuer 1974). Denoting by  $p_1(C)$  the differential distribution of expected counts (i.e.,  $p_1(C) \sim C^{-(\beta+1)}$  for  $C > C_0$ ), the characteristic function  $p_1(\omega)$  of  $C$  is given by

$$p_1(\omega) = \int_{C_0}^{\infty} p_1(C) \exp(i\omega C) dC. \tag{8}$$

As long as  $C_0 > 0$  and  $\beta > 1$  this integral converges and yields  $p_1(\omega) = \beta (-i\omega C_0)^{\beta} \Gamma(-\beta, -i\omega C_0)$ , where  $\Gamma(a, z)$  denotes the complementary incomplete  $\Gamma$ -function as usual. For convenience let us define a modified  $\Gamma$ -function in which a factor  $z^{-a}$  is absorbed, i.e.  $\hat{\Gamma}(a, z) \equiv z^{-a} \Gamma(a, z)$ . Furthermore,  $p_N(\omega) \equiv \exp\{N[p_1(\omega) - 1]\}$ , where in this definition  $N$  is an arbitrary constant, which in our case becomes  $N = K \Omega_{\text{eff}}$ . The probability  $\hat{p}_N(C)$  of obtaining the number of counts  $C$  is given by the Fourier transform of  $p_N(\omega)$ :  $\hat{p}_N(C)$  is the probability distribution of the expected number of counts which is not observed directly in X-ray astronomy, but rather convolved with a Poisson distribution, and so statistical fluctuations due to counting statistics may enlarge or diminish the “intrinsic” background fluctuations. Let therefore the expected total number of (unfluctuated) background counts per beam be given by  $B$ . This background can be thought of being composed of the

mean cosmic (truly) diffuse background as well as backgrounds produced locally (i.e., particle events and scattered solar X-rays). The total background  $B_{\text{total}}$  consists of a fluctuating and non-fluctuating background component,  $B_{\text{total}} = B + C$ . Interpreting  $B$  as the mean value of the unfluctuated background and  $C$  as the fluctuated (Poisson) mean background, both measured *per pixel*, the probability  $p(n)$  to observe  $n$  counts in a beam is then given by

$$p(n) = \int_0^\infty dC \left[ \frac{(B + C)^n}{n!} e^{-(B+C)} \right] \hat{p}_N(C). \quad (9)$$

$p(n)$  finally represents the probability to observe  $n$  counts in the solid angle  $\Omega_{\text{eff}}$ , given the parameters  $B$ ,  $\beta$ ,  $K$  and  $C_0$ . The integrals in Eq.(9) can be solved using the residue theorem (cf. Freyberg & Schmitt 1998). Also a recurrence relation can be obtained such that the  $\hat{\Gamma}$ -function has to be computed just once. Since the probability distributions can be computed analytically this method is suitable for a wide range of applications. Freyberg & Schmitt (1998) discuss the fluctuations in the new SXRb all-sky maps with  $12'$  resolution and bright point sources masked (Snowden et al. 1997).

For practical use we rearranged the parameters of the distribution, the mean  $\langle B_{\text{total}} \rangle$  of the total background in counts, and the fraction  $\xi = \frac{\langle C \rangle}{\langle B_{\text{total}} \rangle}$  of the fluctuated background  $\langle C \rangle$  of the total background  $\langle B_{\text{total}} \rangle$ . Tests of this method have been performed with non-cosmic background components such as the PSPC particle background ( $\beta \sim 4.2$  and  $\xi < 0.01$ ) and scattered solar X-rays. Also pointed observations (much longer exposure) can be used for this analysis. In the  $3/4$  keV band best maximum likelihood fit parameters at  $b^{\text{II}} \sim 20^\circ$  were  $\beta \sim 1.6$  and  $\xi \sim 0.12$ . At higher galactic latitudes  $\xi$  tends to increase while at lower latitudes  $\xi$  decreases. At  $1/4$  keV we obtained  $\beta \sim 2.0$  and  $\xi \sim 0.05$ , at  $1.5$  keV  $\beta \sim 1.5$  and  $\xi \sim 0.35$ . In the  $3/4$  keV band similar values are expected from the extragalactic background. Therefore it appears unlikely that much of the excess  $3/4$  keV X-rays is due to point sources. Besides point-like *sources* also small-scale *absorption* variations (clouds, holes) enter the fluctuation distribution. While extra clouds cause lower counts than expected holes in the interstellar medium can be related to "sources". The angular scales of  $1'$  used in our analysis of pointed observations can be converted to spatial scales of  $1$  pc if we assume a distance of  $60$  pc. Recent observations and models of the local neutral interstellar medium have shown inhomogeneities even on scales  $< 0.01$  pc (e.g., Diamond et al. 1989, Marscher et al. 1993, Meyer & Blades 1996, Elmegreen 1997, Vergely et al. 1997). This has not been discussed here in detail and will be presented in a later work.

## 5 Summary

In our short report we have given an overview of the analysis of the  $3/4$  keV SXRb. In particular, we have developed a new computational scheme

for fluctuation analysis. Point sources do not appear to dominate the 3/4 keV band excess. Multipole analysis has revealed a dipole similar to the C/B ratio found in the Wisconsin surveys. We favour spatial variations of a distant hot plasma component (galactic halo). However, X-ray colours do not exclude additional temperature changes of the distant component or a multi-component distant emission.

## References

- Abramowitz M., Stegun I. (eds.), 1965, *Handbook of Mathematical Functions*, Dover, New York
- Breitschwerdt D., Egger R., Freyberg M.J., Frisch P.C., Vallergera J.V., 1996, *Space Sci.Rev.* 78, 183
- Diamond P.J., Goss W.M., Romney J.D., Booth R.S., Kalberla P.M.W., Mebold U., 1989, *ApJ* 347, 302
- Elmegreen B.G., 1997, *ApJ* 477, 196
- Fabian A.C., Barcons X., 1992, *ARA&A* 30, 429
- Freyberg M.J., 1994, PhD Thesis, LMU München
- Freyberg M.J., 1996, in "The Physics of Galactic Halos", H. Lesch, R.-J. Dettmar, U. Mebold, R. Schlickeiser (eds.), Akademie-Verlag Berlin, p.117
- Freyberg M.J., Schmitt J.H.M.M., 1998, *in preparation*
- Giacconi, R., Bechtold, J., Branduardi, G., Forman, W., Henry, J.P., Jones, C., Kellogg, E., van der Laan, H., Marshall, H., Murray, S.S., Pye, J., Schreier, E., Sargent, W.L.W., Seward, F., Tananbaum, H.: 1979, *ApJ* 234, L1
- Kuntz K.D., Snowden S.L., Verter F., 1997, *ApJ* 484, 245
- Lukacs E., 1970, *Characteristic Functions*, 2<sup>nd</sup> ed., Griffin, London
- Marscher A.P., Moore E.M., Bania T.M., 1993, *ApJ* 419, L101
- McCammon D., Burrows D.N., Sanders W.T., Kraushaar W.L., 1983, *ApJ* 269, 107
- McCammon D., Sanders W.T., 1990, *ARA&A* 28, 657
- Meyer D.M., Blades J.C., 1996, *ApJ* 464, L179
- Morrison R., McCammon D., 1983, *ApJ* 270, 119
- Raymond J.C., Smith B.W., 1977, *ApJSS* 35, 419
- Scheuer P.A.G., 1957, *Proc. Cambridge Philos. Soc.* 53, 764
- Scheuer P.A.G., 1974, *MNRAS* 166, 329
- Schmitt J.H.M.M., Snowden S.L., 1990, *ApJ* 361, 207
- Snowden S.L., Schmitt J.H.M.M., Edwards B.C., 1990, *ApJ* 364, 118
- Snowden S.L., 1996, in "Proc. of the International Conference on *Röntgenstrahlung from the Universe* in Würzburg", eds. H.U. Zimmermann, J.E. Trümper & H. Yorke, MPE Report 263, 299
- Snowden S.L., Egger R., Freyberg M.J., McCammon D., Plucinsky P.P., Sanders W.T., Schmitt J.H.M.M., Trümper J., Voges W., 1997, *ApJ* 485, 125
- Snowden S.L., Egger R., Finkbeiner D.P., Freyberg M.J., Plucinsky P.P., 1997, *ApJ* (*accepted*)
- Wang Q.D., 1997, these proceedings
- Worrall D.M., Marshall F.E., Boldt E.A., Swank J.H., 1982, *ApJ* 255, 111
- Vergely J.-L., Egret D., Freire Ferrero R., Valette B., Köppen J., 1997, in "Hipparcos - Venice '97", ed. B. Battrick, ESA SP-402, p.603